# Control system design for the starch mashing phase in the production of beer

Alberto Leva Filippo Donida
Politecnico di Milano, Dipartimento di Elettronica e Informazione
Via Ponzio, 34/5 - 20133 Milano, Italy

## Abstract

The starch mashing phase, the first one in the brewing process, has a fundamental influence on the quality of the final product. In particular, a good temperature control can significantly reduce the product variability, and also improve the process efficiency by (slightly) reducing the mashing phase duration. In this work, control-oriented models of the mashing process, including biochemical reactions' representation and energy balance equations, are used to synthesise and test some temperature control schemes. The mix of equation- and algorithm-based modelling allowed by Modelica allows to size the control equipment to the (nearly) final detail, including for example the comparison of different types of heating actuators.

*Keywords: brewing; process control; process/control co-simulation*

## 1 Introduction

Many models were proposed in the literature for the starch mashing phase in the brewing process, mostly with the aim of understanding the underlying biochemistry, and therefore correctly sizing the necessary equipment. This manuscript continues the previous work [7], where a well-established literature model (that given its purpose however takes the mash temperature as an exogenous variable) was complemented with suitable energy equations, so as to obtain a new model suitable for simulation studies aimed at the synthesis of the necessary temperature control. Based on said model, two studies are illustrated, First, the temperature profile typically used (that at present comes essentially from heuristic considerations) is re-designed so as to obtain the required final product composition with a (slightly) shorter mashing phase, to the advantage of process throughput and energy efficiency. Then, the control system is simulated both as a continuous-time system and including a (quasi-)*replica* model of the control code: in particular, the possibility of employing an on-off heating actuator instead of a modulating one is investigated, so that the devised control solution can be applied in the presence of realistic equipment.

## 2 The mashing model

The mashing model used here is based on the work by [2]. Through the enzymatic activity and the consequent degradation of the starch, the carbohydrates production is evaluated; the phenomenon is ruled by the amount of fermentable sugars (glucose, maltose, and maltotriose) that constitute the nourishment base for the yeast during the fermentation phase, and also by non-fermentable sugars (dextrins), that participate in the process, as shown by the equations later on. Through the knowledge of the initial compound of the barley malt (i.e., initial amount of sugar and dextrins, starch concentration, and amylase potential) and of the initial mash temperature, it is possible to determine the enzymatic activity and the carbohydrates concentration dynamics—see works such as [6, 3] for deeper discussions on the matter.

The key part of the model is in the prediction of the starch hydrolysis, since that phenomenon determines the quantity of fermentable carbohydrates in the wort, and therefore the alcoholic degree of the finally obtained beer. As for that particular reaction, the objective of mashing is to reach the maximal fermentable carbohydrates productivity, subject to a convenient (and frequently product-specific) specification on the final dextrins concentration (i.e., non-fermentable carbohydrates) so as to ensure the organoleptic

© The Modelica Association, 2009

DOI: 10.3384/ecp09430083

qualities of the beer. The starch is firstly gelatinised, and then transformed into fermentable sugars (sucrose, maltose, and maltotriose) and non-fermentable sugars (dextrins) through the enzymatic activity. Note that also part of the dextrins will be transformed into fermentable sugars.

Obviously, gelatinisation is not an instantaneous phenomenon, since it depends on the concentration of the involved reactants. It therefore depends on temperature, and if temperature is taken as exogenous, its only dynamics comes from mass (concentration) balances; in that framework, the starch gelatinisation kinetic is represented as a first-order reaction. From some experiments it is noticed in the literature that at a given temperature $T_g$ (typically around 60°C) a discontinuity is present in the phenomenon; to deal with that problem, the starch gelatinisation rate $r_g$, expressed in $g/kg\,s$, is traditionally modelled by two alternative equations, namely

$$r_g = k_{g1} \exp\left(-\frac{E_{g1}}{RT}\right)[S_s] \quad for\ T < T_g \tag{1}$$

and

$$r_g = k_{g2} \exp\left(-\frac{E_{g2}}{RT}\right)[S_s] \quad for\ T > T_g, \tag{2}$$

where $[Ss]$ is the ungelatinised starch concentration ($g/kg\ of\ mash$); $E_{g1}$, $E_{g2}$ the activation energy ($J/mol$); $k_{g1}$, and $k_{g2}$ the pre-exponential factor ($s^{-1}$); $T$ the temperature ($K$) of the mash; $T_g$ the threshold temperature ($K$) and $R$ the gas constant ($8.31 J/mol\ K$). The relationship between the global enzymatic activity and the temperature may be represented as the composition of two terms: the temperature effect on the specific activity of each one enzyme site, and the coupled time-temperature effect on the denaturation of active sites. This leads to

$$r_{de\alpha} = k_{d\alpha} \exp\left(-\frac{E_{de\alpha}}{RT}\right)[E_\alpha] \tag{3}$$

and

$$r_{de\beta} = k_{d\beta} \exp\left(-\frac{E_{de\beta}}{RT}\right)[E_\beta], \tag{4}$$

where $r_{de}$ is the reaction rate ($U/kg\,s$) of denaturation, $[E_\alpha]$ and $[E_\beta]$ the active site concentrations ($U/kg\ of\ mash$), $E_{de\alpha}$ and $E_{de\beta}$ the activation energies ($J/mol$) for the denaturation and $k_{d\beta}$ and $k_{d\beta}$ the pre-exponential factors ($s^{-1}$). The global enzyme activation rate ($r_{ac}$ expressed in $U/kg\,s$) can be represented by

$$r_{ac\alpha} = k_{d\alpha} \exp\left(\frac{-E_{de\alpha}}{RT}\right)[E_\alpha]\, a_\alpha \tag{5}$$

and

$$r_{ac\beta} = k_{d\beta} \exp\left(\frac{-E_{de\beta}}{RT}\right)[E_\beta]\, a_\beta, \tag{6}$$

where $a_\alpha$ and $a_\beta$ are the enzymatic site specific activities, that can be approximated by a suitable polynomial in the temperature range of interest (we omit details for brevity). The chemical reactions for the hydrolysis of starch and dextrins into glucose, maltose, and maltotriose are

$$\begin{gathered}
(C_6H_{10}O_5)_n + n(H_2O) \rightarrow n(C_6H_{12}O_6) \\
(C_6H_{10}O_5)_n + \frac{1}{2}n(H_2O) \rightarrow \frac{1}{2}n(C_{12}H_{22}O_{11}) \\
(C_6H_{10}O_5)_n + \frac{1}{3}n(H_2O) \rightarrow \frac{1}{3}n(C_{18}H_{32}O_{16}) \\
(C_6H_{10}O_5)_n \rightarrow x(C_6H_{10}O_5)_{n/x} \\
(C_6H_{10}O_5)_{n/x} + \frac{n}{x}n(H_2O) \rightarrow \frac{n}{x}n(C_6H_{12}O_6) \\
(C_6H_{10}O_5)_{n/x} + \frac{n}{2x}n(H_2O) \rightarrow \frac{n}{2x}n(C_{12}H_{22}O_{11}) \\
C_6H_{10}O_5)_{n/x} + \frac{n}{3x}n(H_2O) \rightarrow \frac{n}{3x}n(C_{18}H_{32}O_{16})
\end{gathered} \tag{7}$$

According to the reaction scheme (7) and the specific action of $alpha-$ and $beta-$amylases, the kinetics for the gelatinised starch hydrolysis (expressed in $g/kg\ s$) into glucose, maltose, maltotriose and dextrins are, respectively, represented by

$$r_{gl} = k_{gl} a_\alpha [S_g] \tag{8}$$

$$r_{mal} = k_{\alpha,mal} a_\alpha [S_g] + k_{\beta,mal} a_\beta [S_g] \tag{9}$$

$$r_{mlt} = k_{mlt} a_\alpha [S_g] \tag{10}$$

$$r_{dex} = k_{dex} a_\alpha [S_g] \tag{11}$$

and similarly, the kinetics for the dextrins hydrolysis is given by

$$\acute{r}_{gl} = \acute{k}_{gl} a_\alpha [D] \tag{12}$$

$$\acute{r}_{mal} = \acute{k}_{\alpha,mal} a_\alpha [D] + \acute{k}_{\beta,mal} a_\beta [D] \tag{13}$$

$$\acute{r}_{mlt} = \acute{k}_{mlt} a_\alpha [D] \tag{14}$$

where $k_{gl}$, $k_{mlt}$, $k_{\alpha,mal}$, $k_{\alpha,mal}$, $k_{dex}$, $\acute{k}_{gl}$, $\acute{k}_{mlt}$, $\acute{k}_{\alpha,mal}$, $\acute{k}_{\beta,mal}$ are the kinetic factors ($kg/U\,s$), $[D]$ and $[S_g]$ the dextrins and the gelatinised starch concentrations ($g/kg\ of\ mash$), and $a_\alpha$ and $a_\beta$

© The Modelica Association, 2009

are the real activity of *alpha* and *beta* amylase ($U/kg\,of\,mash$). Finally, the ordinary differential equations

$$\frac{d[S_s]}{dt} = -r_g \tag{15}$$

$$\frac{d[S_g]}{dt} = r_g - r_{gl} - r_{mal} - r_{mlt} - r_{dex} \tag{16}$$

$$\frac{d[D]}{dt} = r_{dex} - \acute{r}_{gl} - \acute{r}_{mal} - \acute{r}_{mlt} \tag{17}$$

$$\frac{d[gl]}{dt} = -r_{gl} + \acute{r}_{gl} \tag{18}$$

$$\frac{d[mal]}{dt} = -r_{mal} + \acute{r}_{mal} \tag{19}$$

$$\frac{d[mlt]}{dt} = -r_{mlt} + \acute{r}_{mlt} \tag{20}$$

express the carbohydrate concentration evolutions.

Starting from the above work, the objective here is to create models suitable for system studies related to control. It is therefore not appropriate to take the mash temperature as an exogenous variable (as is instead correct, according to the literature, for bio-chemical only studies). On the other hand, for our purposes the temperature dynamics has to be described based on the power generations and exchanges involved in the process, namely the heat released to the tank wall from the external in order to warm up the mass, the heat lost towards the external environment, and the heat coming from the saccharification reactions. Such an extension causes a notable increase of the model complexity, and to maintain that complexity to an acceptable level for system studies, we have to introduce a few assumptions. In detail,and quite reasonably for a system study, we assume that the wort is perfectly mixed, with homogeneous temperature and concentrations, specific heat and density of the components are constant in the considered range of temperature, and the heat contribution of the mechanical mixing actions are negligible.

The typical commercial tanks used have very different sizes and geometries. However, for this study, the tank is assumed to be a vertical cylinder (therefore yielding results immediately suitable also for a home-brewing context, incidentally); the exchange area ($A$) is the sum of the area of the wall around the cylinder plus the area of the bottom, and the net power entering in the wort contained in the vessel (in $W$) is

$$Q = Q_{rea} + Q_{exc} \tag{21}$$

where $Q_{rea}$ is the power generated by the mashing process (obviously with its sign, as mashing is actually an endothermic reaction), and $Q_{exc}$ the power exchanged with the wall and through the wort surface in contact with the air. The energy equation is therefore

$$Q = C_{mass}\frac{d(T_m)}{dt} \tag{22}$$

where $T_m$ is the temperature (in $K$) of the mash and $C_{mass}$ is the heat capacity (in $J/K$) of the mash

$$C_{mass} = M_{water}Cp_{water} + M_{grain}Cp_{grain} \tag{23}$$

with $M_{water}$ and $M_{grain}$ respectively the mass (in $kg$) of the water and the grains, and $Cp_{water}$ and $Cp_{grain}$ the specific heat (in $J/kg\,K$) of the water and the grain. The net power exchanged by the mash is a sum of a two terms, i.e.,

$$Q_{exc} = Q_{mw} + Q_{ma} \tag{24}$$

where $Q_{mw}$ is the heat exchanged with the reactor wall and $Q_{ma}$ is the heat exchanged by the mash in contact with the air above the mash,

$$Q_{ma} = U_{ma}A_{sup}(T_{ext} - T_m) \tag{25}$$

where $U_{ma}$ is the overall heat transfer coefficient (in $W/m^2\,K$) between the mash and the air above, referred to a bulk air temperature as usual in similar cases; $A_{sup}$ is the exchange area (in $m^2$) on the top of the mash ($A_{sup} = \pi r^2$) and $T_{ext}$ is the external temperature (in $K$) of the environment where the tank is located, and

$$Q_{mw} = U_{mw}A_{wall}(T_{wall} - T_m) \tag{26}$$

where $U_{mw}$ is the overall heat transfer coefficient between the mash and the reactor wall; $A_{wall}$ is the exchange area, and $T_{wall}$ is the temperature of the reactor wall. As for the reactor wall temperature, apparently another energy equation is needed, i.e.,

$$C_{wall}\frac{d(T_{wall})}{dt} = Q_{we} - Q_{mw} \tag{27}$$

where $Q_{we}$ is the heat exchanged by the wall in contact with the external air and $C_{wall}$ is the heat capacity of the reactor wall

$$C_{wall} = M_{reactor}Cp_{metal} \tag{28}$$

© The Modelica Association, 2009

with $M_{reactor}$ the mass (in $kg$) of the reactor and $Cp_{metal}$ the specific heat (in $J/kg\,K$) of the metal which compose the tank. The overall mashing reaction is endothermic, thus needs heat to take place. This heat ($Q_{rea}$) is taken away from the mash is the sum of three terms: the power generated by the glucose production $Q_{glu}$, by the maltose production $Q_{mal}$ and by the maltotriose production $Q_{mlt}$.

$$Q_{rea} = Q_{glu} + Q_{mal} + Q_{mlt} \tag{29}$$

For brevity, we report here only the equations for the power originating from the glucose production; those related to maltose and maltotriose are analogous. The power generated by a reaction is typically in the form

$$Q_{reaction} = -ReactionRate * ReactionEnthalpy \tag{30}$$

where the enthalpy of reaction $H$ is the sum of the products' enthalpies minus the reactants' enthalpies.

$$H = H_{prod} - H_{reac}. \tag{31}$$

This enthalpy is however a *standard enthalpy*, calculated in a standard condition (atmospheric pressure and 25°C). This is not our case since the mash temperature is variable. Thanks to the Kirchhoff's equation, we can calculate the reaction enthalpy considering the condition of our process. Kirchhoff's equation (for the glucose production) is represented by

$$H_{reac} = H0_{reac} + C_{glu}\Delta T \tag{32}$$

where $\Delta T = T_m - T_0$ with $T_0$ the standard temperature (25°C) and $T_m$ the mash temperature; $C_{glu}$ is the specific heat capacity of reaction; $H0_{reac}$ is the enthalpy of the reaction in the standard condition which is (looking 31) equal to

$$H0_{glu} = Hf_{glu} - Hf_{water} - Hf_{starch} \tag{33}$$

As for $C_{glu}$, it is the difference between the sum of the specific heat capacities of the products and of the reactants ($Cp_{prod} - Cp_{reac}$), thus

$$C_{glu} = Cp_{glu} - Cp_{water} - Cp_{starch} \tag{34}$$

and of course, the same calculations can be done also for the maltose and maltotriose production. The main part of the Modelica implementation of the so derived model is shown below.

```
//--- energy balances --------------------------------
  Cmash*der(Tm) = Qmash_air + Qmash_tank + Qreact;
  Cmash = Mwater*CpWater + Mgrains*CpMalt;
  Qmash_air = Umash_air*SupArea*(Te - Tm);
  Qmash_tank = -Qbp-Qbb;

  Clat*der(Tlat) = Qbp + Qpe + Qbap;
  Clat = CpMetal*MvessLat;
  Qbp = LatArea *Umash_tank*(Tm - Tlat);
  Qpe = LatArea *Utank_outside*(Te - Tlat);
  Qbap = (pi*radO^2-pi*radI^2)*lambda_m/Lrifbp
         *(Tbase-Tlat);

  Cbase*der(Tbase) = Qbb + Qbe + Q_gasburner - Qbap;
  Cbase= CpMetal*MvessBase;
  Qbb=SupArea*Umash_tank*(Tm - Tbase);
  Qbe=SupArea*Utank_outside*(Te - Tbase);

  radO=radI+LatThick;
  volume = radI^2*pi*level;
  volume = Mwater/densWater + Mmalt/densMalto;
  ContactArea = pi*radI^2 + level*radI*2*pi;
  SupArea = radI^2*pi;
  LatArea =level*radI*2*pi;
  MvessLat=2*radI*pi*H*LatThick *densMetal;
  MvessBase=radI^2*pi*BaseThick *densMetal;


//--- reaction powers --------------------------------
  Qreact = Qglu + Qmal + Qmlt;
  Qglu = -((Rgl + R1gl)*Mgrains)*Hglu;
  Hglu = HOglu/mmGlu + Cglu*(Tm - T0);
  HOglu = HfGlu - HfWater - HfStarch;
  Cglu = CpGlu - CpStarch - CpWater;
  Qmal = -((Rmal + R1mal)*Mgrains)*Hmal;
  Hmal = HOmal/mmMal + Cmal*(Tm - T0);
  HOmal = HfMal/2 - HfWater/2 - HfStarch;
  Cmal = CpMal/2 - CpStarch - CpWater/2;
  Qmlt = -((Rmlt + R1mlt)*Mgrains)*Hmlt;
  Hmlt = HOmlt/mmMlt + Cmlt*(Tm - T0);
  HOmlt = HfMlt/3 - HfWater/3 - HfStarch;
  Cmlt = CpMlt/3 - CpStarch - CpWater/3;

//--- mass balances ----------------------------------
  M = Mwater + Mmalt;
  Mmalt = Mcarbo + Mother;
  Mcarbo = Mglu + Mmal + Mmlt + MstarchGel
           + MstarchNG + Mdex;
  Mother = ((1 - AmIni - GluIni - MalIni - MltIni
            - DexIni)*Mgrains);
  Mglu = Mgrains*glu;
  Mmal = Mgrains*mal;
  Mmlt = Mgrains*mlt;
  MstarchGel = Mgrains*Sg;
  MstarchNG = Mgrains*Ss;
  Mdex = Mgrains*D;
  TotProd = glu + mal + mlt + D - GluIni - MalIni
            - MltIni - DexIni;

//--- sugars' creation rates -------------------------
  Rg = Kg*Ss;
  Kg1 = kg1*exp(-Eg1/(R*Tm));
  Kg2 = kg2*exp(-Eg2/(R*Tm));
  s = arctan((Tm - Tg)*kk)/pi + 0.5;
  Kg = Kg1*(1 - s) + Kg2*s;
  Rgl = kgl*RealActAlfa*Sg;
  Rmal = kamal*RealActAlfa*Sg + kbmal*RealActBeta*Sg;
  Rmlt = kmlt*RealActAlfa*Sg;
  Rdex = kdex*RealActAlfa*Sg;
  R1gl = k1gl*RealActAlfa*D;
  R1mal = k1amal*RealActAlfa*D + k1bmal*RealActBeta*D;
  R1mlt = k1mlt*RealActAlfa*D;
  der(glu) = Rgl + R1gl;
```

© The Modelica Association, 2009

```
  der(D) = Rdex - R1gl - R1mal - R1mlt;
  der(mal) = Rmal + R1mal;
  der(mlt) = Rmlt + R1mlt;
  der(Sg) = Rg - Rgl - Rmal - Rmlt - Rdex;
  der(Ss) = -Rg;
  der(Ealfa) = -RdeAlfa;
  der(Ebeta) = -RdeBeta;

//--- enzimatic activities ---------------------------
  RdeAlfa = KdeAlfa*exp(-EdeAlfa/(R*Tm))*Ealfa;
  RdeBeta = KdeBeta*exp(-EdeBeta/(R*Tm))*Ebeta;
  RealActAlfa = aalfa*Ealfa;
  RealActBeta = abeta*Ebeta;
  aalfa = if aalfa < 0 then 0
     else if Tm < 315 then 1
     else 1.3333333e-07*(Tm -300)^6 - 2.2e-05
          *(Tm - 300)^5+ 0.00144333333333*(Tm - 300)^4
          - 0.0490499999999 *(Tm - 300)^3
          + 0.92383333333122*(Tm - 300)^2
          - 8.89999999997759*(Tm - 300)
          + 34.299999999904;
  abeta = if abeta < 0 then 0
      else if Tm < 304 then 1
      else if Tm >= 304 and Tm < 336
           then 0.049*Tm - 13.9
      else if Tm >= 336 and Tm < 343
           then -0.374*Tm + 128.23
      else 0;
```

In accordance with the notation introduced and used above, the reported code should be practically self-explanatory.

## 3 Mashing temperature control

Temperature control plays a decisive role for the decomposition of malts, and is therefore crucial for beer qualities such as stability and taste [5], while bing also of interest for the overall brewing process, see e.g. [4]. Sticking however to the mashing process, the saccharification temperature control should track the required set point curve (prespecified based on the ingredients and the desired product characteristics, so that it can be thought of as a recipe *datum*) quickly, accurately and without overshoots during the temperature rise; the same control should also exhibit good load disturbance rejection properties, so as to rapidly lead the temperature back to the setpoint should the system exhibit any error caused by external disturbances.

A mashing kettle normally has a large volume, and therefore the temperature dynamics is a lag-dominant process. Given that, generally, many breweries control the temperature by a standard PID algorithm, or similar ones, the main differences residing in the actuation mechanism, see e.g. [1]; we therefore adhere to that approach while structuring our schemes.

The first scheme considered is a single-loop temperature control. To enhance the significance of the study, the scheme is applied to the mashing phase, with the dimensions of the vessel compatible with a home brewing case, where simple controls are more likely to be used than in industrial brewing. In the typical home brewing mashing vessel (with a volume of say 25 litres), the available heating actuator is a gas burner, placed below the vessel base, and fed through a modulating valve (see later on for considerations on the possible use of on/off actuators, however, form more realistic a setting); the available thermal power from such an actuator is about 5 kW.

At first, we can introduce some slight modifications to the mashing vessel model in order to account for the fact that heat is only released to the bottom of the vessel. The walls exchange heat with the external air, but also with the heated vessel bottom. For the vessel base we thus have:

$$C_{base} = M_{base} Cp_{Metal} \quad (35)$$

$$C_{base}\frac{d(T_{base})}{dt} = Q_{fb} + Q_{gasb} + Q_{be} - Q_{bap} \quad (36)$$

with $M_{base}$ the mass (in $kg$) of the reactor's base, $T_{base}$ its temperature and $Cp_{metal}$ the specific heat (in $J/kg\,K$) of the metal which composes the tank; $Q_{fb}$ is the heat exchanged between the mash and the base; $Q_{gasb}$ the power contribution from the gas burner, $Q_{be}$ the heat exchanged with the external environment and $Q_{bap}$ the heat exchanged with the tank wall. For the vessel wall, instead, we have

$$C_{wall} = M_{wall} Cp_{Metal} \quad (37)$$

$$C_{wall}\frac{d(T_{wall})}{dt} = Q_{fw} + Q_{we} + Q_{bap} \quad (38)$$

where $M_{wall}$ is the mass of the reactor's wall and $T_{wall}$ its temperature; $Q_{we}$ the heat exchanged with the external environment. To notice how rightly the power $Q_{bap}$ pass by vessel's base through the wall; $Q_{bap}$ is the heat exchanged between the base of the vessel and the wall, written as

$$Q_{bap} = (\pi r_O^2 - \pi r_I^2)\frac{\lambda_m}{L_{rif}}(T_{base} - T_{wall}) \quad (39)$$

where $r_O$ and $r_I$ are respectively the internal and external radius of the vessel, then the first term represents the annulus formed by the difference between the internal and external circumferences;

© The Modelica Association, 2009

$\lambda_m$ the thermal conductivity of the metal (typically aluminium or steel) and $L_{rif}$ the reference length for the heat exchange. $Q_{fb}$ and $Q_{fw}$ are given by

$$Q_{fb} = U_{fb}A_{base}(T_m - T_{base}) \quad (40)$$
$$Q_{fw} = U_{fw}A_{wall}(T_m - T_{wall}) \quad (41)$$

where $U_{fb}$ and $U_{fb}$ are respectively the overall heat transfer coefficient between the mash and the reactor base and between the mash and the reactor wall; $A_{base}$ the area of the base given by $A_{base} = \pi r_I^2$ and $A_{wall}$ the area of the wall given by $A_{wall} = 2r_I\pi H$, with $H$ the wort level. Finally we have to calculate the heat exchanged by the tank with the outside. This is the sum of two terms:

$$Q_{be} = U_{be}A_{base}(Te - T_{base}) \quad (42)$$
$$Q_{we} = U_{we}A_{wall}(Te - T_{wall}) \quad (43)$$

where $U_{be}$ and $U_{we}$ are the overall heat transfer coefficient between the base and the outside and between the wall and the outside; $Te$ the outside temperature. Then, the heat lost by the mash is

$$Q_{loss} = Q_{ma} - Q_{fb} - Q_{fw} \quad (44)$$

where $Q_{ma}$ is the heat exchanged by the mash in contact with the air above.

$$Q_{ma} = U_{ma}A_{sup}(T_{ext} - T_m) \quad (45)$$

where $U_{ma}$ is the overall heat transfer coefficient (in $W/m^2\,K$) between the mash and the air above; $A_{sup}$ the exchange area on top of the mash. We assume for simplicity here that the heat released by the burner itself to the vessel is related to the heater command by the first order transfer function

$$G(s) = \frac{\mu}{1+Ts} \quad (46)$$

Notice how simple it is, with the proposed approach, to devise quite accurate a model, easy to parametrise with dimensional data, and suitable for control studies. Control examples are reported later on, using as controller blocks an analogue PI with antiwindup, a digital PID in the ISA form with antiwindup and tracking, and a digital ISA PI(D) with antiwindup, tracking, and on-off (time division) output, the Modelica code for the first and third of said controller blocks (the second is a mere restriction of the third) is shown below.

```
model PI
  parameter Real CSmax=1;
  parameter Real CSmin=0;
  parameter Real k=0.7;
  parameter Real Ti=280;
  parameter Real b=0;
  Real SPf;
  Real xRff;
  Real fbOut;

public
  Modelica.Blocks.Interfaces.RealInput PV;
equation
  CS = max(CSmin, min(CSmax, k*(SPf-PV) + fbOut));
  Ti*der(fbOut)+fbOut= CS;
  Ti*der(xRff)+xRff = (1-b)*SP;
  SPf = b*SP+xRff;
public
  Modelica.Blocks.Interfaces.RealInput SP;
  Modelica.Blocks.Interfaces.RealOutput CS;
initial equation
  SPf = SP;
end PI;
model digital2dofPID_TDO
  parameter Real K = 1 "Gain";
  parameter Real Ti = 10 "Integral time [s]";
  parameter Real Td = 0 "Derivative time [s]";
  parameter Real N = 5 "Derivative filter ratio [#]";
  parameter Real b = 1 "SP weight in P action [#]";
  parameter Real c = 0 "SP weight in D action [#]";
  parameter Real CSmax = 100 "Maximum CS";
  parameter Real CSmin = 0 "Minimum CS";
  parameter Real TDsteps = 100 "TDO resolution";
  parameter Real Ts = 0.1 "Sampling time [s]";
  Real counter;
//protected
  Real sp;
  Real spo;
  Real dsp;
  Real pv;
  Real pvo;
  Real dpv;
  Real dp;
  Real di;
  Real d;
  Real dold;
  Real dd;
  Real cs;
  Real cso;
  Real dcs;
  Real StepsUp;
public
  input Modelica.Blocks.Interfaces.RealInput SP;
  input Modelica.Blocks.Interfaces.RealInput PV;
  output Modelica.Blocks.Interfaces.RealOutput CS;
  Modelica.Blocks.Interfaces.RealInput TR;
  Modelica.Blocks.Interfaces.BooleanInput TS;
algorithm
  when sample(0,Ts/TDsteps) then
       counter := counter+Ts/TDsteps;
         if counter>=Ts then
            // Compute control signal
            counter :=0;
            sp := SP;
            pv := PV;
            dsp := sp-spo;
            dpv := pv-pvo;
            if not TS then
               dp := K*(b*dsp-dpv);
               di := K*Ts/Ti*(sp-pv);
               d  := (Td*pre(d)+K*N*Td*(c*dsp-dpv))
                     /(if Td>0 then Td+N*Ts else 1);
               dd := d-dold;
```

© The Modelica Association, 2009

```
            dcs := dp+di+dd;
            cs := cso + dcs;
          else
            cs := pre(TR);
          end if;
          if cs>CSmax then
             cs:=CSmax;
          end if;
          if cs<CSmin then
             cs:=CSmin;
          end if;
          spo := sp;
          pvo := pv;
          cso := cs;
          dold := d;
          StepsUp := floor
                     ((cs-CSmin)/(CSmax-CSmin)*Ts);
        end if;
        CS := if (counter<StepsUp) then CSmax
              else CSmin;
  end when;
end digital2dofPID_TDO;
```

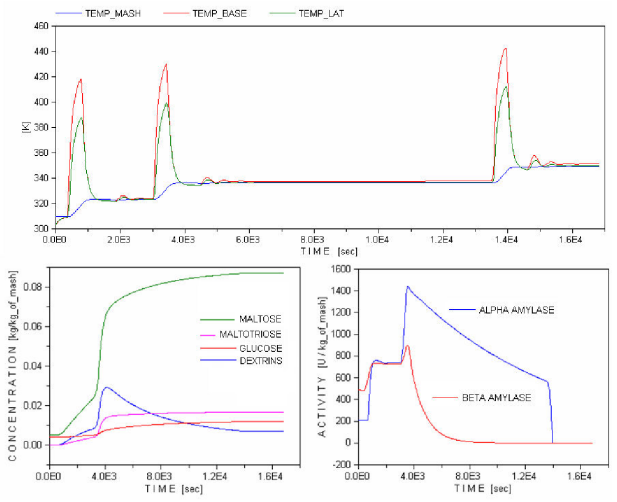


Figure 1: Evolution of the main variables in the gas-burner heated mash. In the first box temperature of the vessel's base, vessel's wall and mash. In the second box the carbohydrate evolutions and in the third one the enzymatic activities.

# 4 Simulation examples

## 4.1 Simulation model assessment

The first example aims at validating the model presented above, that includes both biochemical and energy-related phenomena, with respect to biochemical-only ones, and considering essentially carbohydrates' concentrations and enzymatic activities. To do so, the temperature is controlled via a PI regulator acting on the heating power, and "reasonably" tuned by hand based on some simulated open-loop responses, and the evolution of the variables of interest is compared to that obtained by impressing the temperature (with no energy equation, like in [2]) instead of giving only its set point, and having the temperature determined by energy phenomena.

Figure 1 reports an example of such tests. As can be seen, with a well functioning temperature control, the relevant process variables follow the expected behaviour closely enough, and both carbohydrates' concentrations and enzymatic activities are practically identical to those obtained with the models in [2]. The model presented here can thus be taken as reliable for system studies aimed at control design.

## 4.2 Analogue control

To further witness the obtained results, we now present a mashing simulation where temperature is controlled by a cascade structure, having the heating fluid flow rate as the inner variable, instead of a single loop. In figure 2 an industrial tank is considered, that contains $1000kg$ of water and $300kg$ of grains: through our control structure, we try to have the mash follow the same temperature profile as in the previous simulation (with quite a different plant setup, notice). Observe the good temperature evolution of the mash in response to the reference profile, in particular the correct rise of about 1 $K/min$. A fast and constant rise of the temperature toward the set point is considered important in mashing, which means that the presented control is performing definitely well. As a particular advantage of the cascade structure, we can also show what happens if, upstream of the valve, a significant temperature decrease occurs (before 8000 $sec$, from $417K$ to $390K$, in $10sec$). We can notice how the valve quickly reacts, thanks to the internal loop of the cascade structure; this compensation allows the heating jacket temperature to stay almost constant, and consequently the same to be true for the mash temperature inside the tank. After 10000 $sec$ heating fluid temperature comes back to the previous value. As for the heat exchanges, the thermal energy generation and transfer that influence the mash temperature can be observed. As shown in equations 21 and 24 the mash is affected by lost heat, by the heat produced in the saccharification reaction and by the heat exchange through the tank wall. In figure 3 these thermal powers are shown for the first $100min$ of mashing.

© The Modelica Association, 2009

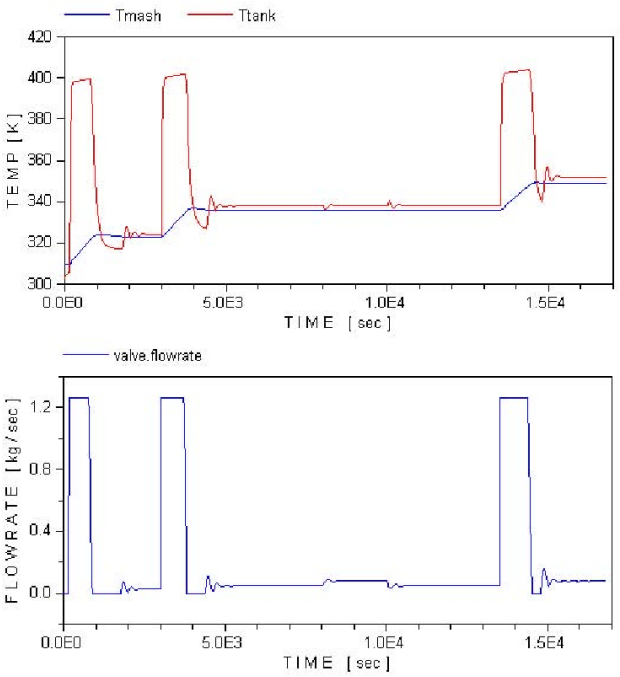


Figure 2: Mashing cascade control.

Having such variables available can apparently be of help for equipment sizing, and overall process and control commissioning.

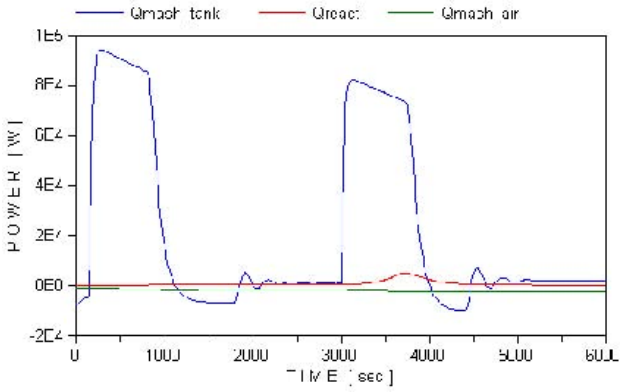


Figure 3: Thermal powers through the mash.

### 4.3 Analogue versus digital control and on-off actuation

In this section we briefly present two simulated versions of a single-loop mashing temperature control scheme, one (entirely in the continuous time) aimed at control law commissioning and/or regulator parameter tuning, the other (hybrid) at control equipment specification and assessment. The diagram of the Modelica model used for the reported test is shien in figure 4.

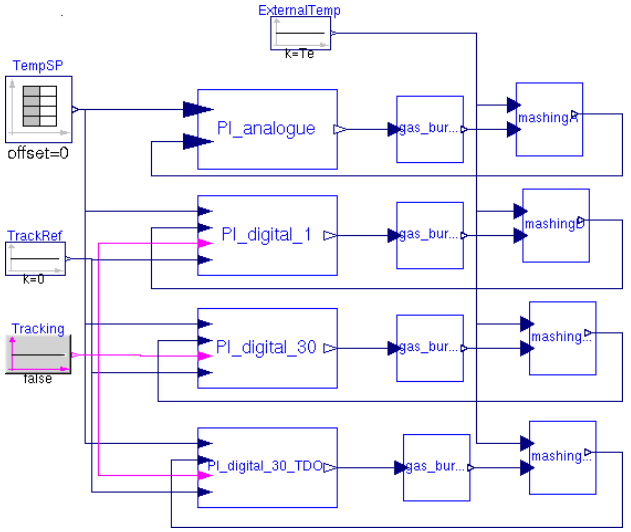


Figure 4: Diagram of the Modelica model used for the simulations on analogue versus digital control, and on-off actuation.

The controller is a PI with normalised gain of 0.6, and an integral time of 340s (the way that tuning was achieved is irrelevant for the scope of this manuscript). Figure 5 shows the results obtained with that PI as an analogue controller and as a digital one, with a sampling tome of 1s (suitable for a modulating actuator) and of 30s (suitable for an on-off one, managed by a time division output as is typically done in such cases). It can be seen that the analogue controller behaves very well, while the other two (hybrid) simulated systems show that the situation can be successfully managed also with the time division controller and the on-off actuator. In addition, some differences in the initial phase are evidenced, that are due to the different way the antiwindup is realised in the analogue and the digital PI. Hence, the presented models allow for an effective simulation, actually useful for both the control law synthesis, and the sizing of the corresponding equipment.

Finally, figure 6 compares, through a hybrid simulation, the PI of figure 5 with sampling time of 30 seconds and its “time division output” version, where the control signal is interpreted as the duty cycle of the activation for an on-off actuator, of course with a base period of 30 seconds. Notice how the conclusions previously drawn are confirmed by this definitely realistic simulation.

© The Modelica Association, 2009


Figure 5: Analogue and digital mashing temperature control: set point and controlled variable (upper plot), control signal (lower plot).

## 5 Conclusions and future work

Literature models of the starch mashing phase in the brewing process were complemented with suitable energy balance equations, so as to make them suitable for the design and the simulation-based assessment of the corresponding temperature controls. Models were implemented in the Modelica language, and verified against literature data. Temperature control schemes were then presented, that were set up with one of those (first principle) models, in order to illustrate the usefulness and practical applicability of the idea. It is worth noticing that the models are suitable for control studies were the overall system is simulated as a continuous-time one, and also as a hybrid one including both time- and event-based controllers, so as to allow both for the tuning of a control law, and the sizing and verification of the corresponding algorithm and equipment.

Future developments will include more extensive use of model-based control techniques, more extensive validations of both the models and the control schemes developed with them, and also the integration of model forecasts and process measurements, to further improve the control performance. The obtained results are also being ported into the OpenModelica environment [8] to foster their diffusion.

## References

[1] E. Alvarez, J.M. Correa, J.M. Navaza, and C. Rivero. Injection of steam into the mashing process as alternative method for the temperature control and low-cost of production. *Journal of Food Engineering*, 43(4):193–196, 2000.

[2] C. Brandam, X.M. Meyer, J. Proth, P. Strehaiano, and H. Pingaud. An original kinetic model for the enzymatic hydrolysis of starch during mashing. *Biochemical Engineering Journal*, 13(1):43–52, 2003.

[3] B. de Andrés-Toroa, J.M. Girón-Sierra, J.A. López-Orozco, C. Fernández-Conte, J.M. Peinado, and F. Garcia-Ochoa. A kinetic model for beer production under industrial operational conditions. *Mathematics and Computers in Simulation*, 48(1):65–74, 1998.

[4] D.A. Gee and W.F. Ramirez. Optimal temperature control for batch beer fermentation. *Biotechnology and Bioengineering*, 31(3):224–234, 1988.

[5] S. Jiliang, Y. Wei, and G. Dexin. Study of compound optimal control for beer saccharification temperature. In *Proc. 26th Chinese Control Conference*, pages 356–359, Zhangjiajie, PR China, 2007.

[6] T. Koljonen, J.J. Hämäläinena, K. Sjöholmb, and K. Pietiläb. A model for the prediction of fermentable sugar concentrations dur-

© The Modelica Association, 2009 

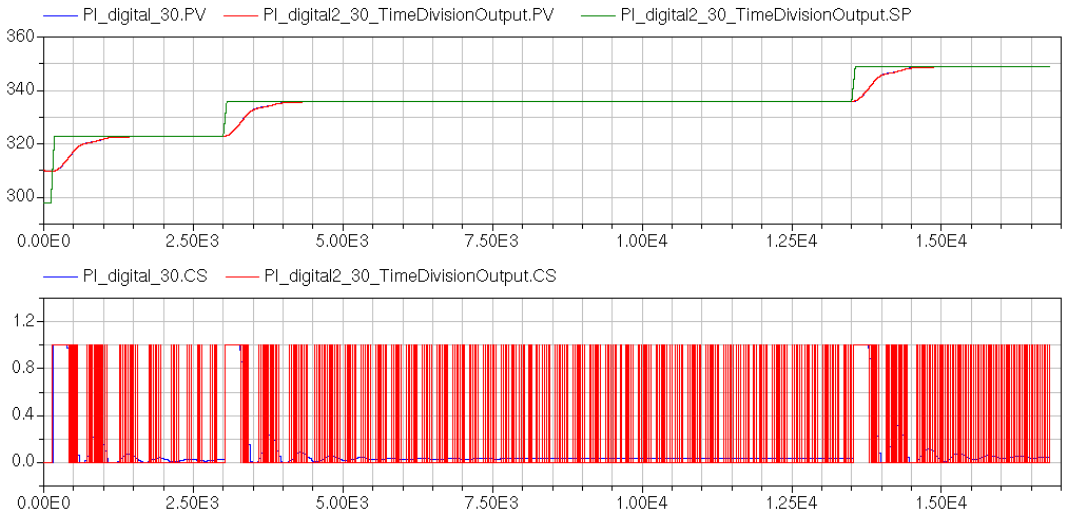


Figure 6: Comparison between the discrete-time and time division output PIs: set point and controlled variable (upper plot), control signal (lower plot).

ing mashing. *Journal of Food Engineering*, 26(3):329–350, 1995.

[7] A. Leva, F. Donida, and M. Bordoni. Object-oriented modelling and simulation of starch mashing. In *Proc. 3rd IFAC Conference on Analysis and Design of Hybrid Systems*, Zaragoza, Spain, 2009.

[8] The Open Source Modelica Consortium. *OpenModelica home page*, 2009. http://www.openmodelica.org.

© The Modelica Association, 2009 